Supporting Information For

New TTF derivatives: several molecular logic gates based on their switchable fluorescent emissions

Chen-Jie Fang, Zhi Zhu, Wei Sun, Chun-Hu Xu, and Chun-Hua Yan*

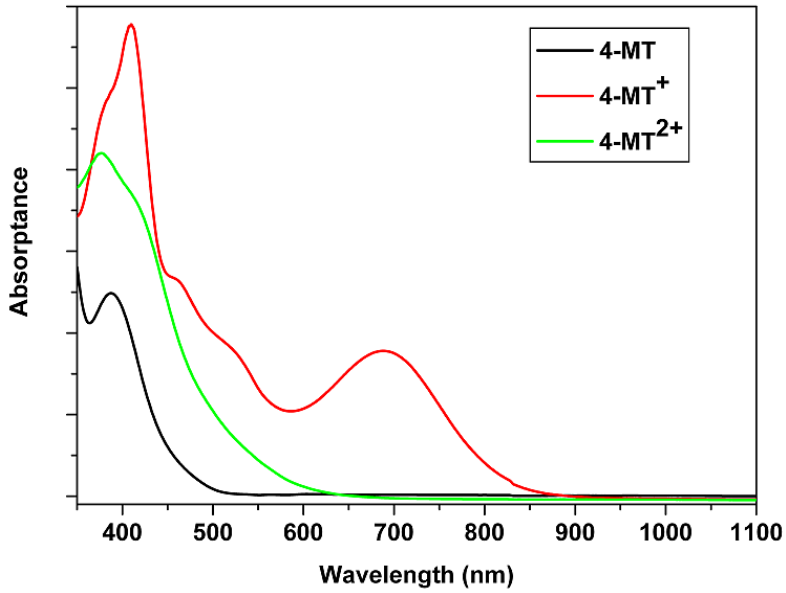

Fig. S1. Absorption of 0.1 mM neutral, cationic and dicationic 4-MT in CH_2Cl_2) upon the addition of $NOBF_4$ in acetonitrile.

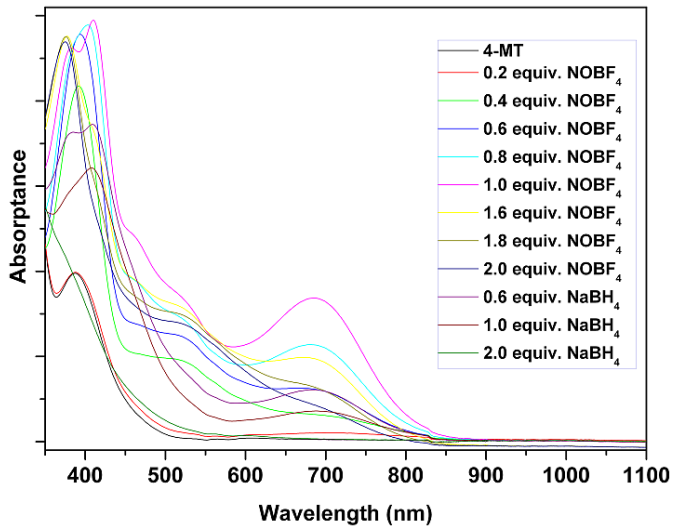

Fig. S2. The evolution of absorption spectra of 0.1 mM 4-MT upon addition of $NOBF_4$ and $NaBH_4$.

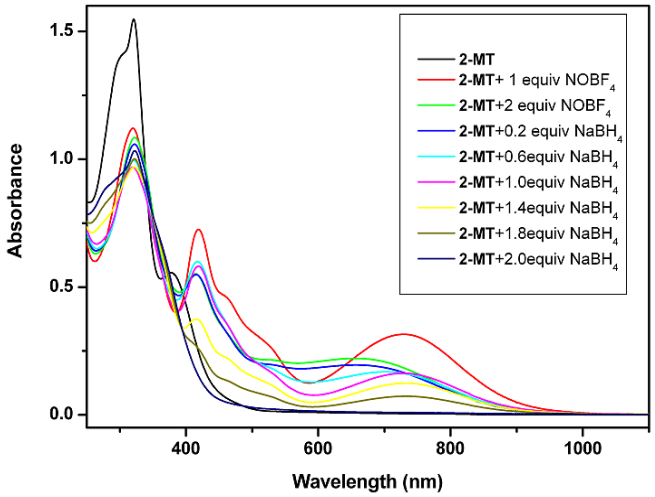

Fig. S3. The evolution of absorption spectra of 5.0×10^{-5} M 2-MT upon addition of $NOBF_4$ and $NaBH_4$.

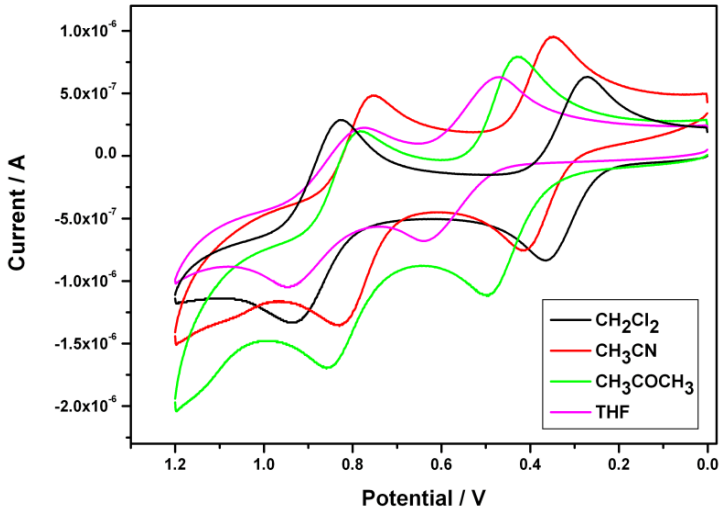

Fig. S4. Cyclic voltammograms of 1×10^{-4} 2-MT in different solvents with 1×10^{-2} Bu_4NPF_6 as supporting electrolyte at a scan rate of 100 mV/s with a Pt disk used as working electrode, a Pt wire as the counter electrode, and a Ag/AgCl electrode as the reference electrode.

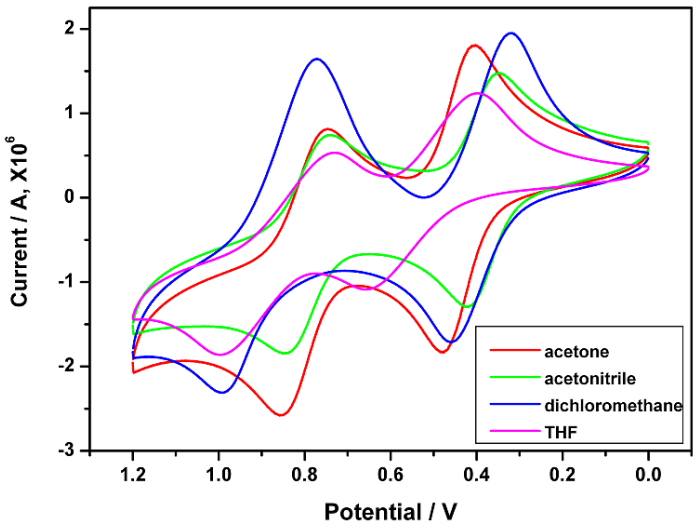

Fig. S5. Cyclic voltammograms of 1×10^{-4} M 4-MT in different solvents with 1×10^{-2} M Bu_4NPF_6 as supporting electrolyte at a scan rate of 100 mV/s with a Pt disk used as working electrode, a Pt wire as the counter electrode, and a Ag/AgCl electrode as the reference electrode.

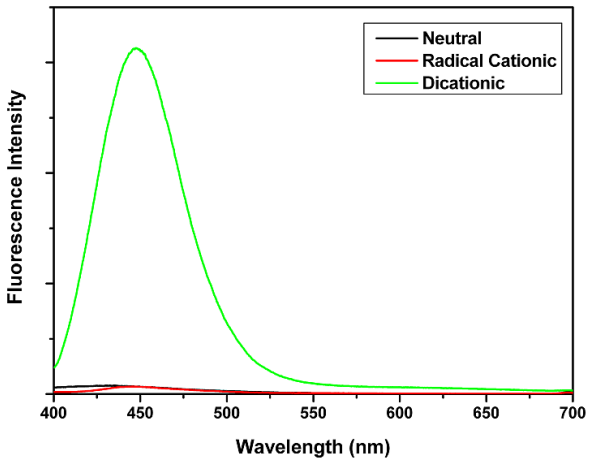

Fig. S6. The fluorescence spectra of neutral, cationic and dicationic 4-MT in CH_2Cl_2.

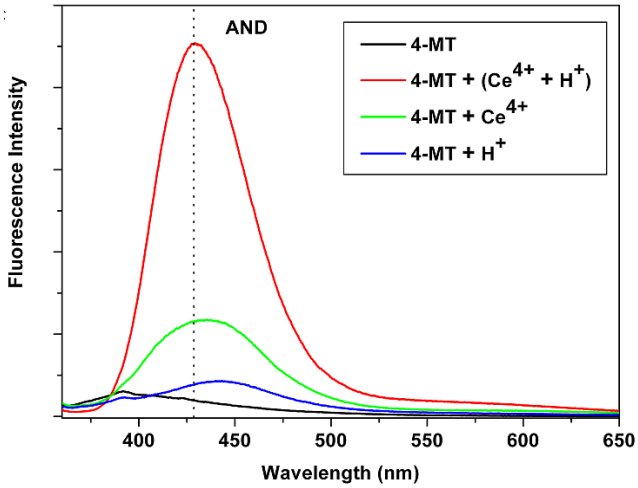

The truth table for AND gate for 4-MT

Ce^{4+}	H^+	PL
0	0	0 (0.04)
1	0	0 (0.26)
0	1	0 (0.09)
1	1	1 (1.00)

Fig. S7. Fluorescence spectra of 4-MT (1.0×10^{-5} M) in CH_2Cl_2 under different input conditions (2.0×10^{-5}M $(NH_4)_2Ce(NO_3)_6$ and 6.5×10^{-5} M CF_3COOH in acetonitrile) and the truth table for AND logic gate. The normalized fluorescence intensities (PL) are shown in the brackets.

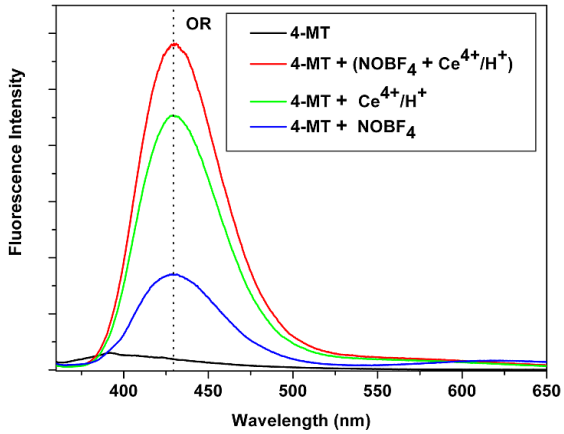

The truth table for OR gate for 4-MT

$Ce^{4+} + H^{+}$	$NOBF_4$	PL
0	0	0 (0.03)
1	0	1 (0.78)
0	1	1 (0.29)
1	1	1 (1.00)

Fig. S8. Fluorescence emission spectra for 4-MT(1.0×10^{-5} M) in CH_2Cl_2 under different input conditions (2.0×10^{-5} M $(NH_4)_2Ce(NO_3)_6$, 6.5×10^{-5} M CF_3COOH and 7.5×10^{-5} M $NOBF_4$ in acetonitrile) and the truth table for OR logic gate. The normalized fluorescence intensities (PL) are shown in the brackets.

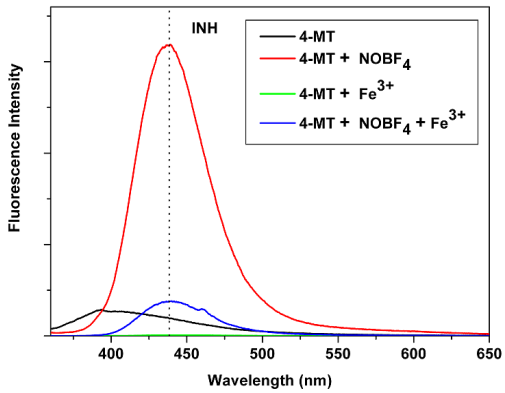

The truth table for INHIBIT gate for 4-MT

Fe^{3+}	$NOBF_4$	PL
0	0	0(0.06)
1	0	0 (0.00)
0	1	1(1.00)
1	1	0(0.12)

Fig. S9. Fluorescence emission spectra for 4-MT(1.0×10^{-5} M) in CH_2Cl_2 under different input conditions (1.5×10^{-4} M $NOBF_4$ and 4.0×10^{-4} M $FeCl_3$ in acetonitrile) and the truth table for INHIBIT logic gate. The normalized fluorescence intensities (PL) are shown in the brackets.

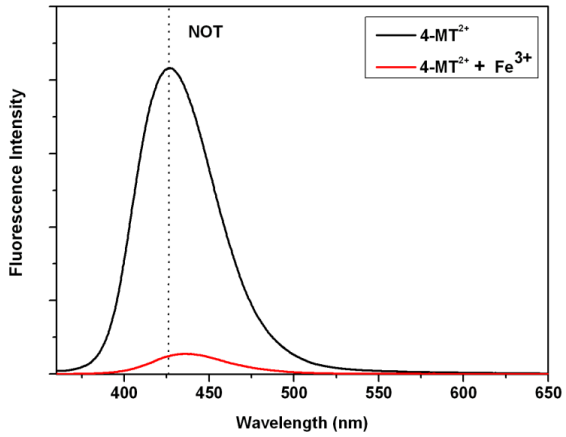

The truth table for NOT gate for 4-MT

Fe^{3+}	PL
0	1(1.00)
1	0(0.06)

Fig. S10. Fluorescence emission spectra for 4-MT^{2+} (1.0×10^{-5} M) in CH_2Cl_2 under input of 4.0×10^{-4} M $FeCl_3$, in acetonitrile and the truth table for NOT logic gate. The normalized fluorescence intensities (PL) are shown in the brackets.

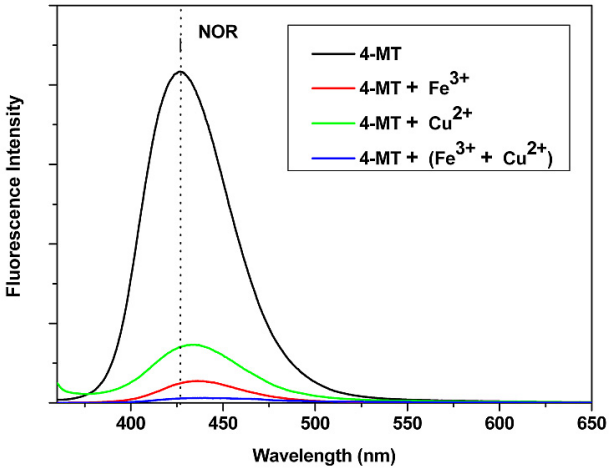

The truth table for NOR gate for 4-MT

Cu^{2+}	Fe^{3+}	PL
0	0	1 (1.00)
1	0	0 (0.17)
0	1	0 (0.06)
1	1	0 (0.00)

Fig. S11. Fluorescence emission spectra for 4-MT^{2+}(1.0×10^{-5} M) in CH_2Cl_2 under different input conditions (4.0×10^{-4} M $FeCl_3$ and 1.6×10^{-3} M $CuCl_2$ in acetonitrile) and the truth table for NOR logic gate. The normalized fluorescence intensities (PL) are shown in the brackets.

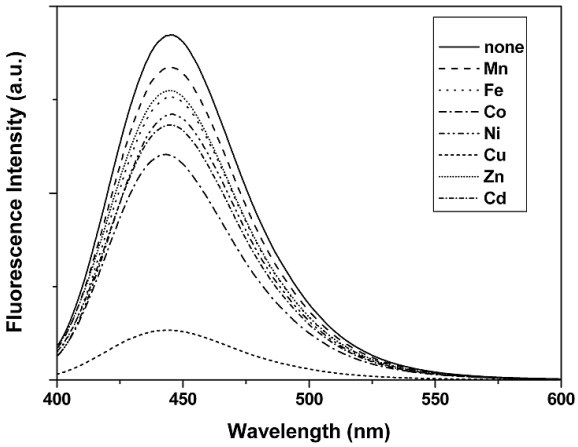

Fig. S12. Fluorescent spectra of 2-MT^{2+} (5.0×10^{-5} M) in CH_2Cl_2 in the presence of various metal ions (1.0×10^{-3} M, in acetonitrile)